

# Site-specific formation of metastable $\text{OCS}^{2+}$ studied by Auger-electron-ion coincidence method

T Kaneyasu<sup>1,3</sup>, M Ito<sup>2</sup>, K Soejima<sup>2</sup>, Y Hikosaka<sup>1,4</sup> and E Shigemasa<sup>1</sup>

<sup>1</sup>UVSOR Facility, Institute for Molecular Science, Okazaki 444-8585, Japan

<sup>2</sup>Department of Environmental Science, Niigata University, Niigata 950-2181, Japan

E-mail: [kaneyasu@saga-ls.jp](mailto:kaneyasu@saga-ls.jp)

Received 30 March 2015, revised 21 April 2015

Accepted for publication 28 April 2015

Published 19 May 2015



CrossMark

## Abstract

We have studied the site-specific formation of metastable  $\text{OCS}^{2+}$  in the C1s and the O1s Auger decays of OCS molecules by using an Auger-electron-ion coincidence technique. The coincidence measurement reveals the metastable character of the Auger final states with the  $(3\pi)^{-2}$  configuration. The formation of metastable  $\text{OCS}^{2+}$  is observed negligibly in the C1s Auger decay and only weakly in the O1s Auger decay, in contrast to the favorable metastable formation previously reported for S2p Auger decay. It is found that the origin of the site-specificity in the formation of metastable  $\text{OCS}^{2+}$  arises from the localization effect of the valence orbital involved in the Auger transition. The dissociative dication states related to individual fragmentation pathways are also derived from the coincidence measurement.

Keywords: metastable dication, Auger decay, electron-ion-coincidence technique

(Some figures may appear in colour only in the online journal)

## 1. Introduction

While doubly-charged molecular ions (dications) are inherently unstable due to the Coulomb repulsion between the nuclei, the existence of metastable molecular dications having lifetimes of the order of at least microseconds has been known from mass spectroscopic studies since the 1930s [1]. The stability and the fragmentation of molecular dications have long been subjects of study in the research field of atomic and molecular physics, and a number of experimental and theoretical works have been carried out [2]. However, details of the electronic structures of molecular dications have been largely unknown until recently because of experimental difficulties in studying the inherently unstable species. Experimental breakthroughs for precise spectroscopic studies on molecular dications were made through efficient electron-electron coincidence techniques such as threshold photoelectron coincidence [3] and time-of-flight photoelectron-

photoelectron coincidence (TOF-PEPECO) [4], both of which can provide dication spectra with vibrational resolution. In particular, the TOF-PEPECO method has been successfully applied to studies of the valence double photoionization of various molecules, and the basic properties of the dication states have been clarified [5].

Besides valence double ionization, molecular dications with two holes in valence orbitals are efficiently produced through Auger decay following core-hole creation in molecules composed of light atoms. The molecular dications thus formed either show metastable character or rapidly dissociate into fragments, depending on the properties of their potential surfaces. Auger electron spectroscopy can provide information on the stability and dissociation properties of the molecular dications [6, 7]. However it is usually difficult to derive detailed dication dynamics from molecular Auger spectra, due to the many overlapping Auger transitions, most of which produce dissociative dication states leading to broad spectral shapes. One promising method for disentangling these complex molecular Auger spectra, and determining the stability and dissociation pathways of the dications, is the coincidence

<sup>3</sup> Present address: SAGA Light Source, Tosu 841-0005, Japan

<sup>4</sup> Present address: Graduate School of Medicine and Pharmaceutical Sciences, University of Toyama, Toyama 930-0194, Japan

observation of energy-selected Auger electrons and product ions [8].

Another important property of molecular Auger decay is the site-specificity in the electronic relaxation process relevant to the localization character of the initial core-hole [9, 10]. With the localized positive charges being preserved in the Auger decay, the subsequent molecular fragmentation often takes place accompanying bond-breaking near the atomic site at which the initial core-hole was created. The Auger-electron-ion coincidence technique has also been applied for studying such site-specific phenomena in detail [11–13]. It is noteworthy that the site-specific formation of the metastable dication following the C1s and O1s Auger decays of CO<sub>2</sub> has been revealed recently by an Auger-electron-ion coincidence method [14].

In this paper, we report a study of the stability and fragmentation of OCS<sup>2+</sup> formed via Auger decay of OCS molecules using the Auger-electron-ion coincidence technique. The dication spectra of low-lying OCS<sup>2+</sup> states have previously been measured by TOF-PEPECO with vibrational resolution [15]. The overall features of the Auger decays, S2p, C1s and O1s Auger spectra, and assignments of the spectral features based on a semi-empirical calculation have also been reported [16]. The effect of the nuclear motion on the Auger transitions has been theoretically studied [17]. Recently, a high-resolution S2p Auger spectrum, and assignments to metastable states on the basis of a theoretical calculation have been reported [7]. Meanwhile, Auger-electron-ion coincidence experiments have been performed only for S2p core-hole creation, and reported in our previous work [18], and later in [19].

In the present work we focus on the Auger decays of OCS following C1s and O1s ionization, in order to elucidate the influence of localized core-holes on the Auger transitions. It is found that the metastable final states are less favored in the Auger transitions subsequent to C1s and O1s ionization, in sharp contrast to the intense production of metastable dications for S2p Auger decay [18–20]. The site-specific formation of metastable OCS<sup>2+</sup> is discussed by combining our previous result for the S2p Auger decay. The present result also clarifies the dissociative dication states which are related to the individual fragmentation processes.

## 2. Experiment

The experiment was performed at the bending magnet beamline BL4B of the UVSOR facility. Synchrotron radiation from the bending magnet was monochromatized to a bandwidth of 0.5 eV by a grazing incidence monochromator. The photon energy scale was calibrated through total ion yield measurements of the inner-shell resonances in OCS. Details of the electron-ion coincidence spectrometer are given in [21, 22]. Briefly, it consists of a double toroidal electron energy analyzer (DTA) [23] and an ion momentum spectrometer, both of which are equipped with time- and position-sensitive detectors (PSDs). The electrons emitted at an angle of 54.7° with respect to the electric field vector of the ionizing

light were analyzed in energy by the DTA. The pass energy of the DTA was set to  $E_{\text{pass}} = 240$  eV. The resolving power of the DTA was estimated to be better than  $E_{\text{pass}}/\Delta E = 100$ . Following the detection of an electron, fragment ions were extracted from the ionization region into the momentum spectrometer by a pulsed electric field. In this study, the pulsed electric field was set to ensure a  $4\pi$ -collection solid angle for fragment ions having kinetic energies less than 5 eV. The electron arrival positions and ion arrival positions and times-of-flight (TOFs) were recorded in list format. The PSD for ions was operated in a multi-hit mode to facilitate the identification of dissociation pathways.

Coincidence data sets were recorded at photon energies of 306 eV and 550 eV for C1s and O1s ionization, respectively. To cover a binding energy range of 25–50 eV in the Auger electron observations, we performed two sets of measurements with different settings of the kinetic energy window of the DTA for each core ionization. Auger electron spectra related to the formation of metastable dications and individual fragmentation pathways were extracted from the coincidence data sets in an off-line analysis in which false coincidence events were carefully subtracted from the raw data. False coincidence rates were estimated from separate measurements in which the pulsed extraction field was triggered by signals from a pulse generator, independent of electron detection.

## 3. Results and discussion

### 3.1. Conventional Auger spectra

Figures 1(a) and (b) show conventional Auger spectra of OCS following C1s and O1s ionization, respectively. These spectra were derived without discrimination by detected ion species from the coincidence data sets. The Auger spectra are plotted on binding energy scales calculated by subtracting the Auger electron energies from the C1s<sup>-1</sup> and O1s<sup>-1</sup> ionization energies of 295.43 and 540.28 eV [16], respectively. The kinetic energy scales are also shown. The spectra exhibit several broad structures resulting from the overlaps of many transitions. We have attached labels to the band structures according to [17]. Although some of the bands, C1, C2, O3, O4, O5 and O6, are not fully resolved in the present study, the measured spectral profile essentially agrees with the previous measurements [16]. The spectral features differ quite significantly from those in the S2p Auger spectrum, which exhibits intense narrow peaks in the binding energy region below 40 eV [16].

The band structures in the Auger spectra can be assigned in detail from the general agreement with the theoretical Auger energies [17]. The calculated energies of the Auger final states with large transition intensities in the C1s and O1s Auger decays are indicated by the vertical bars in figure 1. For the energies indicated, the energy shifts due to nuclear dynamics are taken into account. Note that the valence electronic configuration of the OCS molecule is described as  $(6\sigma)^2(7\sigma)^2(8\sigma)^2(9\sigma)^2(2\pi)^4(3\pi)^4$ . A weak band structure

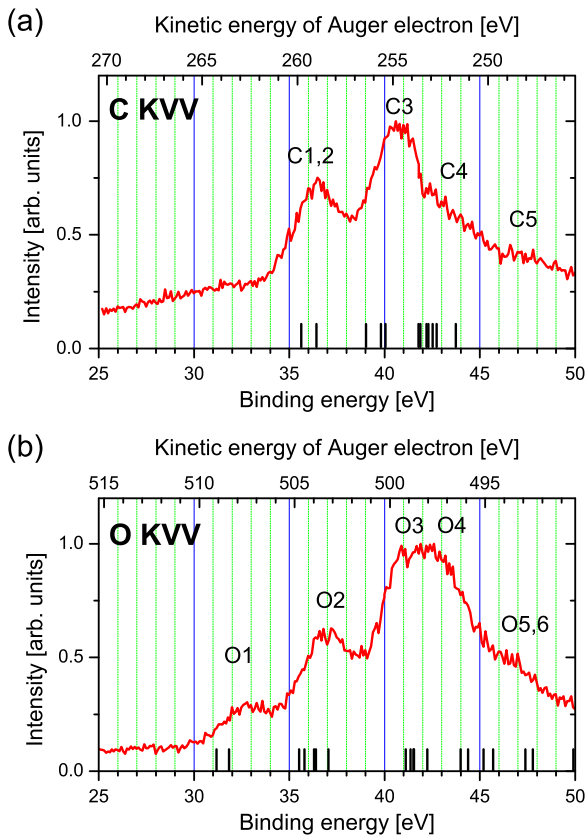


**Figure 1.** (a) C1s and (b) O1s conventional Auger spectra derived from the total events of the coincidence data. Vertical bars indicate the calculated energy positions of the Auger final states with large transition intensities in the C1s and O1s Auger decays [17]. The labels attached in the Auger spectra are adopted from [17].

ranging from 30 to 35 eV is observed only in the O1s spectrum. This lowest band O1 is assigned to the formation of  $(3\pi)^{-2}$  states. In the binding energy region of 35–38 eV, intense band structures are discernible in both spectra. These structures are attributed to the dication states characterized by two-hole configurations; one hole in the  $3\pi$  orbital and the other hole in the  $2\pi$ ,  $9\sigma$ , or  $8\sigma$  orbital. A large number of dication states exist above 38 eV, where both spectra exhibit the most intense band structure; these spectral features are due to the complex overlaps of transitions involving the  $7\sigma$ ,  $8\sigma$ ,  $9\sigma$ ,  $2\pi$  and  $3\pi$  orbitals.

### 3.2. Coincidence Auger spectra

To extract Auger spectra filtered by the coincident detection of metastable dications and other individual fragmentation signatures, which we refer to as coincidence Auger spectra, we discriminate the coincidence events using the ion TOF information. As an example, a one-dimensional TOF spectrum of product ions and a two-dimensional map representing the TOFs of the first-hit and second-hit ions on the detector for C1s Auger decays are shown in figures 2(a) and (b), respectively. The one-dimensional TOF spectrum can be used to determine the ion TOF range necessary to extract the coincidence Auger spectrum related to the formation of

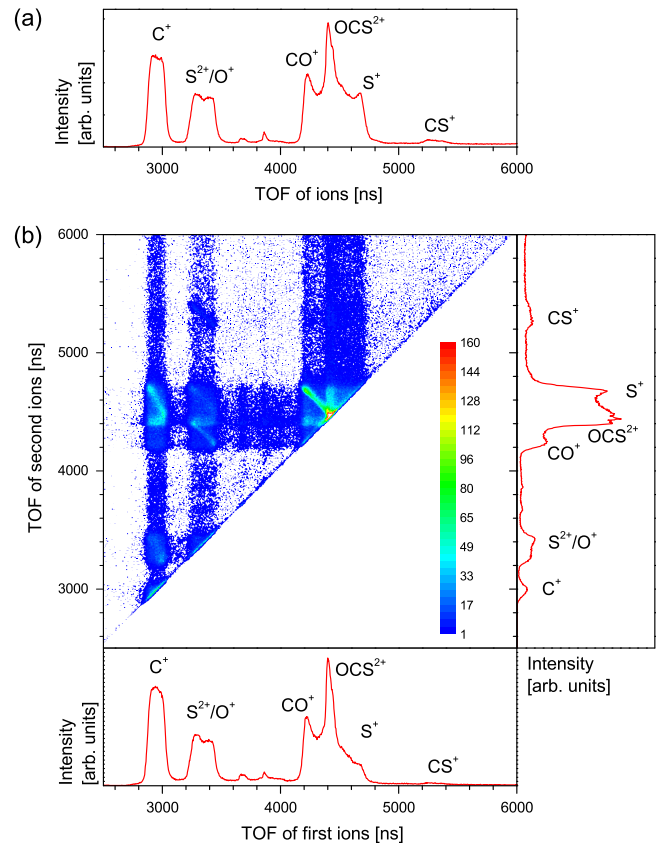


**Figure 2.** (a) One-dimensional TOF spectrum of the product ions measured in coincidence with C1s Auger electrons. (b) Two-dimensional TOF map representing the formations of ion-pairs following C1s Auger decay. Projections of the two-dimensional map are plotted in the bottom and right panels, representing the summed TOF spectra for the first-hit and second-hit ions. Note that the weak TOF peaks observed between 3600 and 4000 ns are due to experimental artifacts.

metastable  $\text{OCS}^{2+}$ , while the two-dimensional TOF map can be used to determine the TOF ranges necessary to select individual ion-pair fragmentation routes. Note that false coincidence events are included in the data plotted in figure 2.

Prior to discussion of the coincidence Auger spectra, we first describe the dissociation mechanisms of  $\text{OCS}^{2+}$  which can be identified from the two-dimensional map. While false coincidence events appear as horizontal and vertical stripes on the two-dimensional map, true coincidences between ion pairs appear as diagonal island structures. The two-body fragmentations into  $\text{CO}^+ + \text{S}^+$ ,  $\text{O}^+ + \text{CS}^+$  and  $\text{CO}^+ + \text{S}^{2+}$  are observed as diagonal structures with slopes of  $-1$ , since the two fragments are emitted in opposite directions with the same momenta. The detection of  $\text{CO}^+ + \text{S}^{2+}$  events resulting from the dissociation of triply charged  $\text{OCS}^{3+}$  can be assumed to be due to false coincidences, since the detection window of the Auger electron energy used here is much lower than the triple ionization threshold of OCS at 60 eV [24]. Three-body fragmentations into  $\text{O} + \text{C}^+ + \text{S}^+$ ,  $\text{O}^+ + \text{C} + \text{S}^+$  and  $\text{O}^+ + \text{C}^+ + \text{S}$  can be identified as diagonal structures with slopes steeper than  $-1$ , indicating that sequential processes play a role in the three-body fragmentation of  $\text{OCS}^{2+}$  [25, 26].

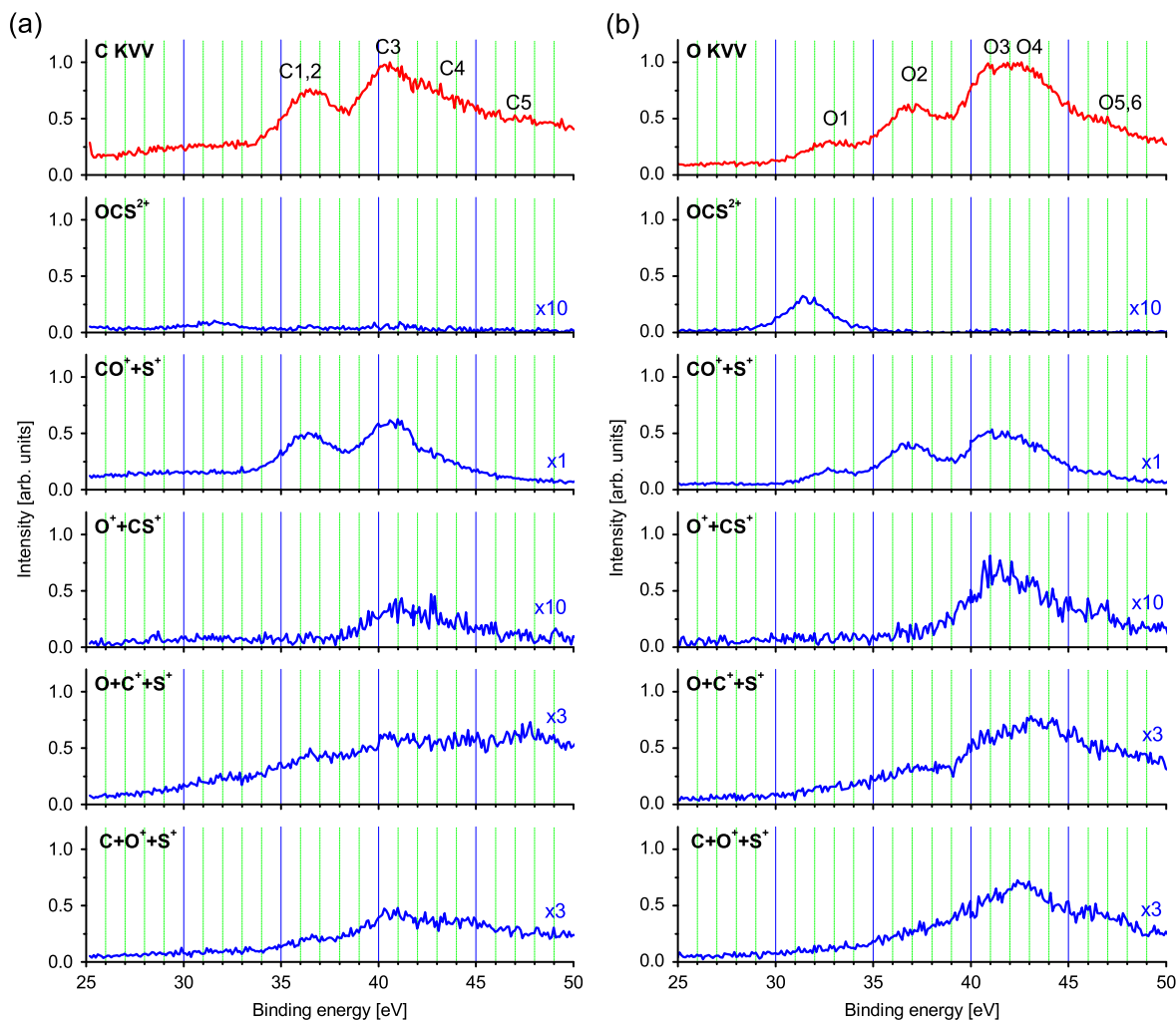


**Figure 3.** Conventional and coincidence Auger spectra of OCS subsequent to (a) C1s and (b) O1s ionization. The coincidence spectra are extracted from the coincidence data sets by filtering the Auger electron signals related to the formation of metastable  $\text{OCS}^{2+}$  and individual fragmentation pathways. The intensities of the coincidence spectra are normalized to the corresponding conventional spectrum.

The coincidence Auger spectra for metastable  $\text{OCS}^{2+}$  and for individual fragmentation pairs are shown in figures 3(a) and (b) for C1s and O1s ionization, respectively. The coincidence Auger spectra for three-body fragmentation to  $\text{O}^+ + \text{C}^+ + \text{S}$  are not presented, since the count rates were too low to reveal any reliable structure in the derived spectra. The coincidence Auger spectra are normalized to the conventional Auger spectra shown in the top panel of each figure, and thus the spectral intensities directly reflect the decay branching ratios.

For both C1s and O1s Auger decay, the coincidence observation reveals the metastable character of the Auger final states lying in the range 30–35 eV, which are attributed to dication states with two holes in the non-bonding  $3\pi$  orbital. In contrast to the intense production of metastable  $\text{OCS}^{2+}$  in S2p Auger decay [18], the metastable final states are less favored in the C1s and O1s Auger decays. This site-specific formation of metastable  $\text{OCS}^{2+}$  is discussed in the next section.

The present observation confirms the dissociative character of the dication states identified in the Auger-electron–

ion coincidence experiment for S2p Auger decay [18]. In general, two-body fragmentation to  $\text{CO}^+ + \text{S}^+$  dominates the dissociation of the dication states lying in the binding energy range 35–45 eV, while the high-lying dication states above 45 eV mainly lead to three-body fragmentation. We here note only the characteristics of the dissociative dication states found in the C1s and O1s Auger decays. For two-body fragmentation to  $\text{CO}^+ + \text{S}^+$ , a small component is observed around 33 eV only in the O1s Auger decay. This weak band structure is peaked at slightly higher binding energy than that related to the metastable dication. Thus this structure can possibly be attributed to Auger decays into vibrationally excited  $(3\pi)^{-2}$  states which pre-dissociate into  $\text{CO}^+ + \text{S}^+$  with a lifetime shorter than the order of microseconds. It is clear that the  $\text{O}^+ + \text{CS}^+$  channel is correlated with the band structures lying above 38 eV for both C1s and O1s Auger decays. In contrast  $\text{O}^+ + \text{CS}^+$  fragmentation is hardly discernible in S2p Auger decay [18] because of the weak population of the dication states above 38 eV. The structures correspond to the overlap of many Auger final states having two holes in the  $7\sigma$ ,  $8\sigma$ ,  $9\sigma$ ,  $2\pi$  and  $3\pi$  valence orbitals. The centers of the band

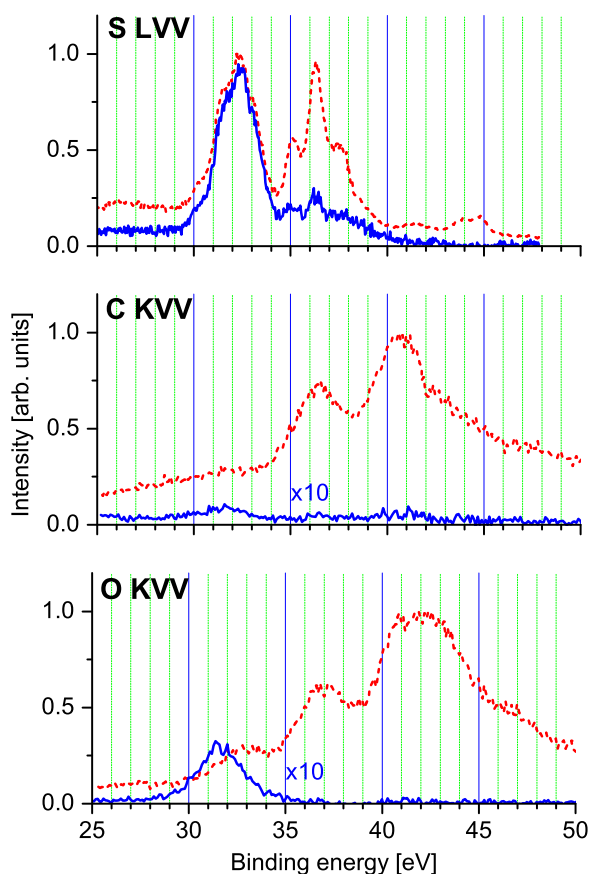


**Figure 4.** Conventional (dashed red lines) and coincidence (solid blue lines) Auger spectra of OCS following C1s and O1s ionization, compared with the corresponding spectra for the S2p ionization [18]. The coincidence spectra are obtained by filtering with the detection of metastable  $\text{OCS}^{2+}$ . The energy resolution for the C1s and O1s Auger spectra is estimated to be  $\Delta E \sim 2.4$  eV, and that for the S2p Auger spectrum  $\Delta E \sim 1$  eV. Note that the binding energy scale for the S2p Auger spectrum is calculated with respect to the ionization energy of the  $\text{S}2\text{p}_{1/2}^{-1}$  core-hole state. The scale is correct for the Auger transitions from the  $\text{S}2\text{p}_{1/2}^{-1}$  state but is shifted by 1.2 eV for those from the  $\text{S}2\text{p}_{3/2}^{-1}$  state.

structures are close to the appearance potential of 42.5 eV in the valence double ionization [27]. The  $\text{OCS}^{2+}$  states related to three-body fragmentations to  $\text{O} + \text{C}^+ + \text{S}^+$  and  $\text{O}^+ + \text{C} + \text{S}^+$  show broad structures above 35 eV, and most three-body fragmentations originate from dication states lying above 40 eV.

### 3.3. Site-specific formation of metastable $\text{OCS}^{2+}$

Next we discuss the mechanism of the site-specificity in the production of the metastable dications. Figure 4 shows the metastable  $\text{OCS}^{2+}$  coincidence Auger spectra and conventional Auger spectra following C1s and O1s ionization, along with the corresponding S2p Auger spectra from our previous study [18]. As mentioned above, the metastable character of the dication states is allocated to the  $(3\pi)^{-2}$  states lying in the binding energy region of 30–35 eV. Note that the binding energy scale for the S2p spectra is calculated with respect to the ionization energy of the  $2\text{p}_{1/2}^{-1}$  core-hole state, while the

Auger decays from the  $\text{S}2\text{p}_{3/2}^{-1}$  and  $2\text{p}_{1/2}^{-1}$  core-hole states (1.2 eV splitting) are overlapped in the Auger spectra. Thus, the metastable  $(3\pi)^{-2}$  structures in the S2p spectra are observed at slightly higher energy than those for the C1s and O1s Auger decays. While the metastable state is barely observed above 36 eV in the C1s and O1s coincidence Auger spectra, the S2p coincidence Auger spectrum shows a sizable intensity in this range. These structures are possibly due to the formation of the bound  $(8\sigma)^{-1}(3\pi)^{-1}$  and  $(2\pi)^{-1}(3\pi)^{-1}$  states identified in the high-resolution Auger spectrum [7]. The weak structure around 35 eV, and part of the peak structure at 36 eV are attributable to an imperfection in the false coincidence subtraction, since there are no metastable states in this energy region.

Here we concentrate on the formation of metastable dication states with two holes at the non-bonding  $3\pi$  orbital. The intensity of the metastable dication state in the S2p Auger decay is much higher than those in the C1s and O1s Auger decays (see figure 4). This site-specific formation of the metastable dications can be qualitatively explained by the spatial distribution of the valence orbital involved in the Auger decay processes. The localization character of the  $3\pi$  orbital can be quantitatively described in terms of the Mulliken population analysis, and the orbital populations have been calculated to be 0.64, 0.32 and 3.04 for around O, C and S atoms, respectively [16]. Due to the localization of the  $3\pi$  valence orbital around the S atom, the valence orbital should show a favorable overlap with the S2p core-hole and thus the S2p core-hole can be preferably filled by a  $3\pi$  electron. Next to the exclusive population around the S atom, the  $3\pi$  orbital is weakly localized around the O atom. Thus a small amount of the metastable dications is observed in the O1s Auger decay while a nearly negligible yield of the metastable dications is produced in the C1s Auger decay. The present observation confirms the interpretations for the localization effect of valence orbitals on the Auger transitions in OCS [16, 17]. We expect that such site-specific phenomena emerge as a general property of the Auger decays involving localized and non-bonding valence orbitals in molecules. Indeed a similar site-specific production of metastable dications has been observed also in the Auger decays of  $\text{CO}_2$  molecules [14].

## 4. Summary

We have studied the site-specific formation of metastable  $\text{OCS}^{2+}$  in the C1s and O1s Auger decays of OCS molecules by using the Auger-electron-ion coincidence technique. The coincidence measurement reveals the metastable character of the Auger final states with a  $(3\pi)^{-2}$  configuration, and the correlations of the dissociative dication states with individual fragmentation pathways. The metastable final states produced following C1s and O1s ionization are populated with much lower probabilities compared to the observation for the S2p ionization. The origin of the site-specificity in the metastable production can be understood in terms of the localization effect of the valence orbitals involved in the Auger transition.

## Acknowledgments

We are grateful to the UVSOR staff for the stable operation of the storage ring. The authors would like to thank Dr J R Harries for critical reading of the manuscript. This work was partially supported by the Japan Society for Promotion of Science, Grant-in-Aid for Scientific Research.

## References

- [1] Vaughan A L 1931 *Phys. Rev.* **38** 1687
- [2] Mathur D 1993 *Phys. Rep.* **225** 193
- [3] Hall R I, McConkey A, Ellis K, Dawber G, Avaldi L, MacDonald M A and King G C 1992 *Meas. Sci. Technol.* **3** 316
- [4] Eland J H D 2003 *Chem. Phys.* **294** 171
- [5] Eland J H D 2009 *Adv. Chem. Phys.* **141** 103
- [6] Püttner R, Liu X J, Fukuzawa H, Tanaka T, Hoshino M, Tanaka H, Harries J, Tamenori Y, Carravetta V and Ueda K 2007 *Chem. Phys. Lett.* **445** 6
- [7] Sekushin V, Püttner R, Fink R F, Martins M, Jiang Y H, Aksela H, Aksela S and Kaindl G 2012 *J. Chem. Phys.* **137** 044310
- [8] Eberhardt W, Plummer E W, Lyo I W, Carr R and Ford W K 1987 *Phys. Rev. Lett.* **58** 207
- [9] Eberhardt W, Sham T K, Carr R, Krummacher S, Strongin M, Weng S L and Wesner D 1983 *Phys. Rev. Lett.* **50** 1038
- [10] Nenner I and Morin P 1996 *VUV and Soft X-ray Photoionization Studies in Atoms and Molecules* ed U Becker and D A Shirley (London: Plenum) p 291 and references therein
- [11] Miron C, Simon M, Leclercq N, Hansen D L and Morin P 1998 *Phys. Rev. Lett.* **81** 4104
- [12] Céolin D *et al* 2005 *J. Chem. Phys.* **123** 231303
- [13] Fukuzawa H, Prümper G, Liu X J, Kukk E, Sankari R, Hoshino M, Tanaka H, Tamenori Y and Ueda K 2007 *Chem. Phys. Lett.* **436** 51
- [14] Hikosaka Y, Shibata Y, Soejima K, Iwayama H and Shigemasa E 2014 *Chem. Phys. Lett.* **603** 46
- [15] Brites V, Eland J H D and Hochlaf M 2008 *Chem. Phys.* **346** 23
- [16] Carroll T X, Ji D and Thomas T D 1990 *J. Electron Spectrosc. Relat. Phenom.* **51** 471
- [17] Minelli D, Tarantelli F, Sgamellotti A and Cederbaum L S 1997 *J. Chem. Phys.* **107** 22
- [18] Kaneyasu T, Ito M, Hikosaka Y and Shigemasa E 2009 *J. Korean Phys. Soc.* **54** 371
- [19] Saha K, Banerjee S B and Bapat B 2014 *Chem. Phys. Lett.* **607** 85
- [20] Feng R, Cooper G, Sakai Y and Brion C E 2000 *Chem. Phys.* **255** 353
- [21] Kaneyasu T, Hikosaka Y and Shigemasa E 2007 *AIP Conf. Proc.* **879** 1793
- [22] Kaneyasu T, Hikosaka Y and Shigemasa E 2007 *J. Electron Spectrosc. Relat. Phenom.* **156-158** 279
- [23] Miron C, Simon M, Leclercq N and Morin P 1997 *Rev. Sci. Instrum.* **68** 471
- [24] Eland J H D, Hochlaf M, Linusson P, Andersson E, Hedin L and Feifel R 2010 *J. Chem. Phys.* **132** 014311
- [25] Eland J H D 1987 *Mol. Phys.* **61** 725
- [26] Ankerhold U, Esser B and Von Busch F 1997 *Chem. Phys.* **220** 393
- [27] Masuoka T and Doi H 1997 *Phys. Rev. A* **47** 278